

## A facilely prepared polypyrrole–reduced graphene oxide composite with a crumpled surface for high performance supercapacitor electrode

Tao Qian,<sup>a</sup> Chenfei Yu,<sup>a</sup> Shishan Wu<sup>\*a</sup> and Jian Shen<sup>ab</sup>Cite this: *J. Mater. Chem. A*, 2013, **1**, 6539Received 21st March 2013  
Accepted 18th April 2013

DOI: 10.1039/c3ta11146f

[www.rsc.org/MaterialsA](http://www.rsc.org/MaterialsA)

A polypyrrole–reduced graphene oxide core–shell composite was facilely fabricated through electrostatic interactions and  $\pi$ – $\pi$  accumulation. This novel composite shows remarkable performance as an electrode material for supercapacitors, with a high specific capacitance of 557 F g<sup>-1</sup> at a current density of 0.5 A g<sup>-1</sup>, and retains a high value after 1000 charge–discharge processes. The maximum energy density of the fabricated supercapacitor based on the mass of active electrodes is calculated to be 49.5 W h kg<sup>-1</sup> and 33.3 W h kg<sup>-1</sup> at a power density of 0.22 kW kg<sup>-1</sup> and 6.06 kW kg<sup>-1</sup>, the improved capacitance might be mainly ascribed to higher conductivity and more crumpled surface of the composite.

Supercapacitors are a promising power source and have potential applications in electronic equipment and hybrid electric vehicles.<sup>1</sup> Based on different energy-storage mechanisms, supercapacitors include electric double layer (EDL) capacitors and pseudo-capacitors. For EDL capacitors, capacitance is mainly enhanced by increasing the surface area of the materials. Carbon materials such as activated carbon, carbon nanotubes, and graphene with high surface area are commonly used for EDL capacitors.<sup>2</sup> Graphene, consisting of a two-dimensional sheet of covalently bonded carbon atoms, has high electronic conductivity, low mass density, extremely high specific surface area,<sup>3,4</sup> and finds a multitude of applications in devices.<sup>5</sup> The high in-plane conductivity and surface area makes it an attractive material for use in supercapacitors.<sup>6</sup> Reduced graphene oxide (RGO), one kind of chemically derived graphene, has shown similar characteristics to graphene in many aspects.<sup>7</sup> RGO crumpled structures may be more complex and intriguing, since the crumple of a structure can change its form/

phase and functionality, which may induce new and distinct properties.<sup>8</sup>

Conductive polymer nanocomposites have become a key area in nanoscience and nanotechnology, offering significant potential in the development of advanced materials in applications such as electronic devices, supercapacitors, rechargeable batteries, functional electrodes, sensors and many other fields.<sup>9</sup> The use of a conductive polymer like polypyrrole (PPy) is particularly promising owing to its high energy storage capacity, good electrical conductivity, ease of low cost synthesis, and environmental stability.<sup>10–12</sup> The existence of positive surface charge on the PPy could provide an interface for the modified materials interaction.

Recently, much effort has been devoted to fabricating composites of PPy and RGO to create a synergetic effect resulting in significantly enhanced performances and stabilities. PPyRGO composites are prepared through various methods including *in situ* polymerization of the monomers in RGO suspensions,<sup>13,14</sup> polymerization of the monomers in graphite oxide (GO) dispersions followed by chemical reduction of GO,<sup>15</sup> electro-polymerization of the monomers on RGO papers,<sup>16</sup> and directly mixing the solution phases of PPy and RGO.<sup>17</sup> It is believed that the RGO surface morphology is important to the performance of supercapacitors. However, little work on modifying the surface morphology of RGO in the composite procedure and investigating the effect of morphology change on capacitive performance has been reported. Herein, we report a facile preparation of a PPyRGO core–shell composite through a two step process (Fig. 1). PPy microspheres with high dispersibility were conveniently synthesized from pyrrole by the initiation of FeCl<sub>2</sub>–H<sub>2</sub>O<sub>2</sub> mixture.<sup>18</sup> GO sheets with negatively charged groups were coated on the PPy microspheres *via* electrostatic interactions (see Fig. S1, ESI<sup>†</sup>) and  $\pi$ – $\pi$  accumulating (see Fig. S2, ESI<sup>†</sup>), the product was then reduced by hydrazine. The prepared PPyRGO core–shell composite could highly disperse in water and shows remarkable performance as the electrode material of supercapacitors.

<sup>a</sup>School of Chemistry and Chemical Engineering, Nanjing University, Nanjing 210093, P. R. China. E-mail: shishanwu@nju.edu.cn

<sup>b</sup>College of Chemistry and Materials Science, Nanjing Normal University, Nanjing, 210097, P. R. China

† Electronic supplementary information (ESI) available. See DOI: 10.1039/c3ta11146f

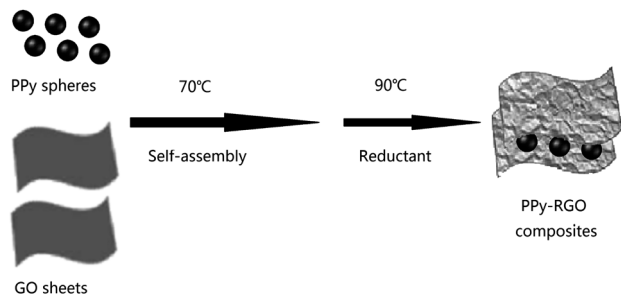


Fig. 1 The route for fabrication of the PPyRGO composite.

To investigate the morphology of the prepared PPyRGO hybrids, SEM and TEM images were taken and the results are shown in Fig. 2. The SEM images (Fig. 2A and B) indicate that the PPy spheres are completely covered with RGO sheets, and the surface of composite film shows typical wrinkle and crumple-like structures compared with pure RGO sheets. More details can be observed from the TEM images (Fig. 2C and D), which show that RGO sheets are coated on the PPy spheres compactly and the scale of spheres is 700–800 nm. HRTEM images were obtained to show the partial morphology of composite. The RGO sheets are obviously crumpled (Fig. 2E) and the thickness is nonuniform in the range 5–10 nm (Fig. 2F). On the basis of experimental results (see Fig. S3, ESI<sup>†</sup>), the size

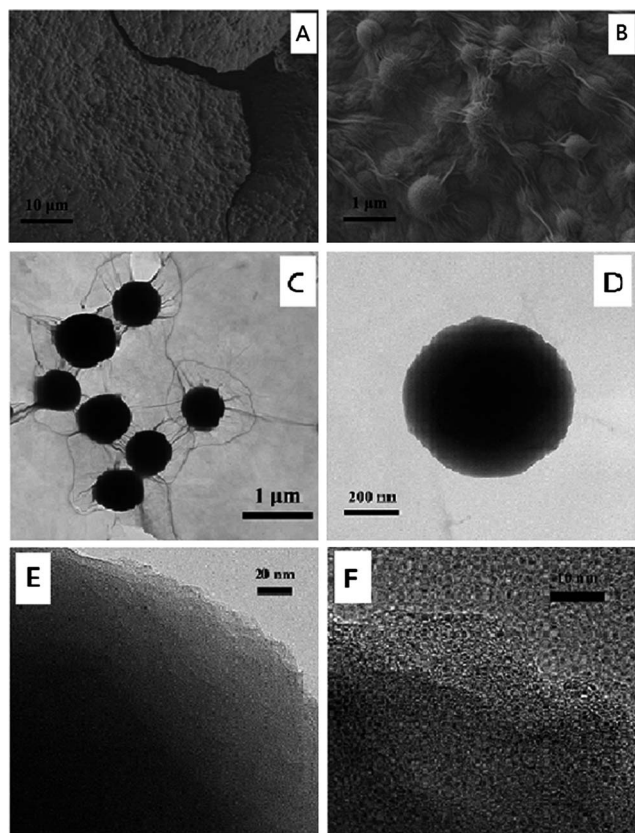


Fig. 2 SEM images of (A) PPyRGO (ratio 1 : 1) composites film, (B) with partial enlarged; TEM and HRTEM images of (C) PPyRGO (ratio 1 : 1) composites, (D–F) with partial enlarged.

of the RGO shell was mainly dependent on the addition of the initial GO sheets as well as the number of layers of the RGO or RGO thickness, and PPyRGO composite films with a weight ratio of 1 : 1 obtained a more crumple and wrinkle surface.

The X-ray diffraction (XRD) data obtained for PPy, GO, PPyGO and the PPyRGO composite are shown in Fig. S4, ESI<sup>†</sup>. The XRD peak of PPy is centered at  $2\theta = 24.1^\circ$ , which is associated with the planar aromatic pyrrole rings. The XRD pattern of GO has a sharp peak centered at  $2\theta = 11.7^\circ$ . After being coated on the PPy microspheres, the characteristic peak of GO at approximately  $11.7^\circ$  could be found in the XRD pattern of the PPyGO composite. As for the PPyRGO composite, a broad peak was strengthened at  $23.3^\circ$  corresponding to RGO was observed, also the characteristic peak of GO at  $11.7^\circ$  disappeared, which means that the GO had been reduced. This result reflects that the RGO sheets are coated on PPy microspheres with electrostatic interactions and  $\pi$ - $\pi$  stacking between them.

The structure of the PPyRGO composite films with different weight ratios was further studied by Raman spectra as shown in Fig. 3. In the Raman spectrum of PPy, the  $1520\text{ cm}^{-1}$  band is assigned to the C=C backbone stretching. The double bands at  $1373$  and  $1290\text{ cm}^{-1}$  are attributed to the ring-stretching mode of PPy. Another double peaks at about  $1012$  and  $954\text{ cm}^{-1}$  are associated with the C-H in-plane deformation. The Raman spectrum of RGO displays two characteristic peaks at  $1358$  and  $1598\text{ cm}^{-1}$  that correspond to the D and G bands respectively. The D/G band intensity ratio expresses the atomic ratio of  $\text{sp}^3/\text{sp}^2$  carbons, which is a measure of the extent of disordered graphite. The intensity ratio of D to G band in the RGO spectrum is calculated to be 0.83, indicating a not completely reduced graphite structure. It is shown that, as the RGO/PPy ratio increases, significant increase in D/G band intensity ratio can be observed. Besides, the double peaks at about  $1012$  and  $954\text{ cm}^{-1}$ , which are associated with the C-H in-plane deformation in PPy, disappear in the PPyRGO spectra. Both of these phenomena imply that RGO sheets are coated on the surface of PPy microspheres successfully.

The electrochemical performance of the samples as the electrode material for supercapacitors was tested by cyclic

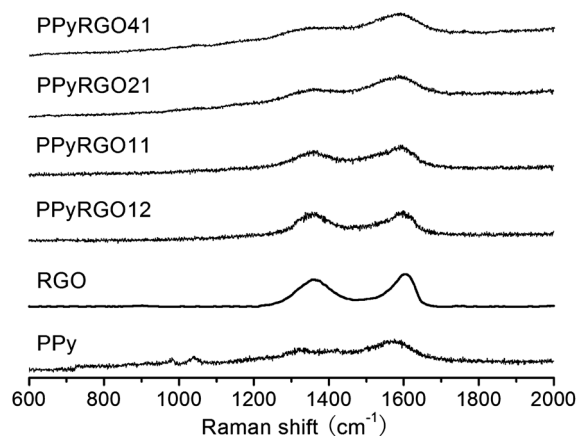


Fig. 3 Raman spectra of PPy, RGO, and PPyRGO composite films with weight ratios of 1 : 2, 1 : 1, 2 : 1 and 4 : 1.

voltammetry (CV) and galvanostatic charge–discharge technique in three-electrode system. Fig. 4 exhibits the CV curves of the PPyRGO11 (indicates that the mass ratio of PPy and RGO is 1 : 1) composite modified electrode with a potential range between  $-0.4$  and  $0.6$  V (vs. SCE) at different scan rates from  $10$  to  $200$   $\text{mV s}^{-1}$ . The shapes of all CV curves show rectangular and symmetric current-potential characteristics, indicating an ideal capacitive behavior. Fig. 5A and B show the galvanostatic charge–discharge curves of PPy.

RGO sheets, and PPyRGO composites modified electrodes at current densities of  $1$   $\text{A g}^{-1}$ , respectively. The near triangular shape of the curves indicates that the composites have good capacitive behaviors. The specific capacitance of the PPyRGO11 is much higher than that of pure PPy and RGO under the same current density, which can be clearly found from the specific capacitance curves. The specific capacitance of the electrode using galvanostatic can be calculated according to the following equation:

$$C_{\text{sp}} = \frac{I\Delta t}{\Delta E m} \quad (1)$$

where  $I$  is the current,  $\Delta E$  is the potential window,  $\Delta t$  is the discharge time, and  $m$  is the mass of active material in a single electrode. As shown in Fig. 5C, the specific capacitance of the PPyRGO11 is the highest ( $430$   $\text{F g}^{-1}$ ,  $1$   $\text{A g}^{-1}$ ) among all the samples, which exceeds that of pure RGO sheets ( $63$   $\text{F g}^{-1}$ ) and PPyRGO composites with other weight ratios, indicating that this ratio is optimal among all the samples. Based on the discussion above, the improved capacitance of the composite might be mainly ascribed to the higher conductivity (see Table S1, ESI†) and more crumpled surface (see Fig. S3, ESI†) of the composite, which can shorten ion diffusion length and allow greater material utilization.

Besides this, it is well-known that an ideal supercapacitor should be able to deliver the same energy under any operation conditions. As a result, it is important to investigate the capacitance retention at a higher current density. The relationships between the  $C_{\text{sp}}$  value and current density measured in a three-electrode system are presented in Fig. 6A, a slight decrease in the  $C_{\text{sp}}$  of PPyRGO11 is observed as the current densities go from  $0.5$  to  $10.0$   $\text{A g}^{-1}$  (about 28%), and  $C_{\text{sp}}$  is maintained quite well under the higher current densities

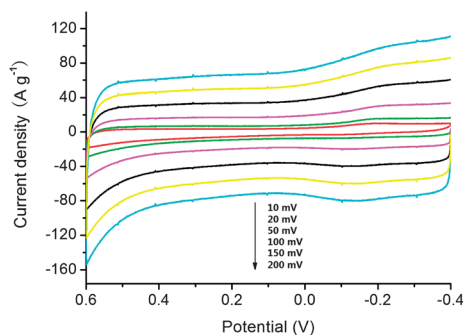


**Fig. 4** CVs of PPyRGO11 supercapacitors in  $1.0$  M KCl solution between  $-0.4$  and  $0.6$  V at different scan rates.

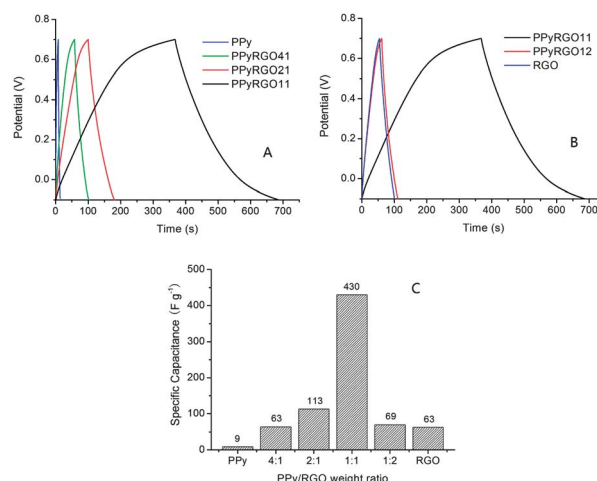


**Fig. 5** (A and B) Galvanostatic charge–discharge curves of different electrodes in  $1.0$  M KCl in a three-electrode system; (C) the specific capacitance of different materials.

(Fig. 6B), indicating that this electrode material exhibits a good capacitance retention capability.

The stability of a supercapacitor during long-term charge–discharge processes is an important property. The capacitive retention of the PPyRGO11 composite was 85% after 1000 cycles (Fig. 6C), indicating a good cycling ability of the composite material. We hypothesize that the PPy spheres stuffing with high dispersion overcomes bulk-quantity aggregation of RGO during the synthesis process. Therefore, the composite materials exhibit a better stability compared with the pristine RGO.

A Ragone plot is a chart used to compare the performance of various energy storing devices.<sup>19</sup> Ragone plots for the devices fabricated with PPyRGO11 are shown in Fig. 5D. The energy density and power density were calculated using galvanostatic charge–discharge data acquired at different current densities. The maximum energy density of the fabricated supercapacitor

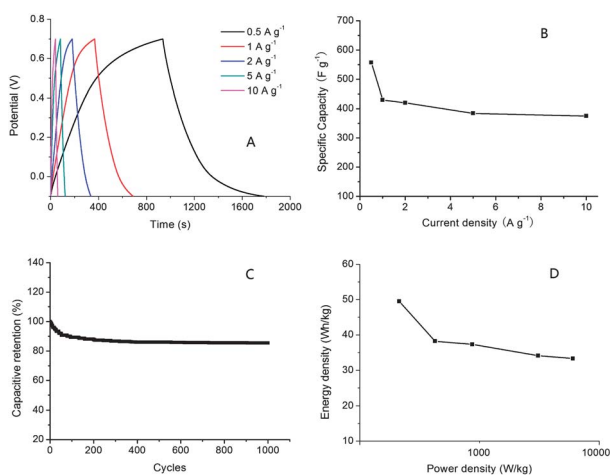


**Fig. 6** (A) Galvanostatic charge–discharge curves of a PPyRGO11 supercapacitor with different current densities; (B) the specific capacitances of a PPyRGO11 modified electrode at different current densities; (C) cycle stability of PPyRGO11 during the long-term charge–discharge process; (D) Ragone plots of PPyRGO11.

based on the mass of active electrodes is calculated to be 49.5 W h kg<sup>-1</sup> and 33.3 W h kg<sup>-1</sup> at a power density of 0.22 kW kg<sup>-1</sup> and 6.06 kW kg<sup>-1</sup>, which exhibit higher energy and power densities than those of other types of commercially available energy storage devices.

In summary, we have fabricated, through a facile route, a PPyRGO core-shell composite, which can be used for the active material of supercapacitor electrodes. The unique features of the composite endow the RGO sheets with abundant crumples. It exhibits excellent specific capacity and cycling stability. The composite with a RGO/PPy mass ratio of 1 : 1 shows a specific capacity of 557 F g<sup>-1</sup> (0.5 A g<sup>-1</sup>), and retains a high value after 1000 charge-discharge processes. The results demonstrate that the prepared composite might be a promising candidate for an electrode material for high performance supercapacitors.

## Notes and references

- 1 J. R. Miller and P. Simon, *Science*, 2008, **321**, 651.
- 2 Y. Gogotsi and P. Simon, *Science*, 2011, **334**, 917.
- 3 A. K. Geim and K. S. Novoselov, *Nat. Mater.*, 2007, **6**, 183.
- 4 K. S. Novoselov, A. K. Geim, S. V. Morozov, D. Jiang, Y. Zhang, S. V. Dubonos, I. V. Grigorieva and A. A. Firsov, *Science*, 2004, **306**, 666.
- 5 Y. C. Si and E. T. Samulski, *Nano Lett.*, 2008, **8**, 1679.
- 6 T. Y. Kim, H. W. Lee, M. Stoller, D. R. Dreyer, C. W. Bielawski, R. S. Ruoff and K. S. Suh, *ACS Nano*, 2011, **5**, 436.
- 7 S. F. Pei and H. M. Cheng, *Carbon*, 2012, **50**, 3210.
- 8 A. Ambrosi, A. Bonanni and M. Pumera, *Nanoscale*, 2011, **3**, 2256.
- 9 H. Kim, A. A. Abdala and C. W. Macosko, *Macromolecules*, 2010, **43**, 6515.
- 10 H. L. Wang, Q. L. Hao, X. J. Yang, L. D. Lu and X. Wang, *Electrochem. Commun.*, 2009, **11**, 1158.
- 11 Q. F. Wu, K. X. He, H. Y. Mi and X. G. Zhang, *Mater. Chem. Phys.*, 2007, **101**, 367.
- 12 C. Zhou and S. Kumar, *Chem. Mater.*, 2005, **17**, 1995.
- 13 X. Zhou, T. Wu, B. Hu, G. Yang and B. Han, *Chem. Commun.*, 2010, **46**, 3663.
- 14 D. Zhang, X. Zhang, Y. Chen, P. Yu, C. Wang and Y. Ma, *J. Power Sources*, 2011, **196**, 5990.
- 15 K. Zhang, L. Zhang, X. Zhao and J. Wu, *Chem. Mater.*, 2010, **22**, 1392.
- 16 A. Davies, P. Audette, B. Farrow, F. Hassan, Z. Chen, J. Choi and A. Yu, *J. Phys. Chem. C*, 2011, **115**, 17612.
- 17 Q. Wu, Y. X. Xu, Z. Y. Yao, A. R. Liu and G. Q. Shi, *ACS Nano*, 2010, **4**, 1963.
- 18 Z. Liu, Y. Liu, S. Poyraz and X. Y. Zhang, *Chem. Commun.*, 2011, **47**, 4421.
- 19 J. aidev and S. Ramaprabhu, *J. Mater. Chem.*, 2012, **22**, 18775.